A Portable Ka-Band Front-End Test Package for Beam-Waveguide Antenna Performance Evaluation—Part I. Design and Ground Tests

T. Y. Otoshi, S. R. Stewart, and M. M. Franco
Ground Antennas and Facilities Engineering Section

As described in previous articles, a unique experimental method was used to test the new Beam Waveguide (BWG) antenna at Deep Space Station 13 in the Goldstone Deep Space Communications Complex near Barstow, California. The methodology involved the use of portable test packages to make measurements of operating noise temperatures and antenna efficiencies (as functions of antenna pointing angles) at the Cassegrain focal point and the final focal point located in a subterranean pedestal room. Degradations caused by the BWG mirror systems were determined by making comparisons of the measured parameters at the two focal points of the antenna. Previous articles were concerned with the design, performance characteristics, and test results obtained with an X-band test package operating at 8.45 GHz. This article discusses a Ka-band test package designed for operation at 32 GHz. Noise temperature measurement results are presented for the Ka-band test package in an "on-the-ground" test configuration.

I. Introduction

Previous articles [1,2] have given detailed descriptions of the test package design, performance characteristics, and test results for the X-band package in "on-the-ground" and "on-the-antenna" test configurations at 8.45 GHz. It was shown that the X-band test package was used successfully to test the new DSS 13 BWG antenna at 8.45 GHz.

This article is the third in a series of reports on the measured performance of the new BWG antenna. In this article, the design of a test package developed for Ka-band is described. In addition, measured operating noise temperatures for the Ka-band test package in the on-the-ground test configuration are presented. A companion article, "Part II," in this issue presents the results of tests performed on the new BWG antenna with the Ka-band test package.

II. Ka-Band Test Package Design

Figure 1 shows the system block diagram of the Ka-band test package. Depicted are typical Cassegrain front-end microwave components, such as a horn, polarizer, round-to-rectangular transition, and a waveguide switch. When the Ka-band WR28 switch is in the antenna path

configuration, the switch connects the horn assembly to a WR28 coupler followed by a cryogenically cooled high-electron-mobility transistor (HEMT) and a downconverter. The insertion loss of the path between the horn aperture and the input of the HEMT at 32 GHz is 0.27 dB ±0.02 dB.

When the switch is in the ambient-load path configuration, the switch connects an ambient thermal reference load to the HEMT. System linearity calibrations are performed with a remotely controlled noise diode assembly. Noise temperature calibrations are performed with an ambient-load thermal reference termination, in which is embedded a digital readout thermometer. For this Ka-band test package, the microwave signal is downconverted to an intermediate frequency (IF) of 60 MHz and sent via a coaxial cable to a power-meter total-power radiometer system.

The requirement of testing the antenna at F1 and F3 required the test package to be convertible from a 29- to 23-dBi horn configuration. The conversion is accomplished through the use of horn extensions of the same taper going from an aperture diameter of about 5.122 in. to 1.986 in. Figures 2 and 3, respectively, are photographs of the fabricated and assembled Ka-band test package in its 29-dBi horn configuration for testing the system on the ground. The test package in the 29-dBi horn configuration, as measured from the bottom of the lower frame to the horn aperture, is about 8.5 ft high, while the 23-dBi configuration is about 14.3 in. shorter.

The Ka-band HEMT assembly shown in Fig. 2 is a four-stage amplifier with an overall gain of 24.4 dB and an effective input noise temperature of 56.6 K. Following the HEMT assembly are waveguide components and a Ka-band downconverter assembly (Fig. 3). A block diagram of the Ka-band downconverter assembly is given in Fig. 4. The vital components of this downconverter assembly are a stainless steel WR28 guide section for thermal isolation, a 32-GHz bandpass filter, a 3.5-dB noise figure mixer, an IF bandpass filter, and a thermoelectric temperature controller. The system operates double sideband, where input signals in the bands (31.89 to 31.99-GHz) and (32.01 to 32.11 GHz) become downconverted to an IF band of 10 to 110 MHz, whose center frequency is 60 MHz.

Early in the development stage, considerable gain instability problems were experienced with the Ka-band downconverter. The problems were finally overcome with the installation of the thermoelectric temperature controller (see Fig. 3), which maintained the temperature inside the downconverter to within ±0.4 deg C. After installation of the thermoelectric cooler, the gain change during a typical day was reduced from 0.95 dB to about 0.13 dB.

The Ka-band noise diode assembly (Fig. 5) provides an injection signal of about 81 K into the HEMT and is used to check system linearity. Measurements of the excess noise injected are made when the waveguide switch is first in the antenna position and then in the ambient load position. The difference in the excess noise measured in the two waveguide positions provides a means for determining noise-temperature measurement-system nonlinearity.

III. Radiometer System

Although the radiometer computer system is not part of the test package, the test package had to be designed specifically to interface with the computer-controlled radiometer system. For either the X- or Ka-band test packages, the downconverted output is sent to the computer-controlled radiometer system via a coaxial cable.

Figure 6 is a block diagram showing the interface between the Ka-band test package and the total-power radiometer system. The IF noise power is measured with a Hewlett-Packard 436A Power Meter. An IBM personal computer sends commands to change the waveguide switch to a thermal reference load position and reads the digital information on the thermal reference load to a resolution of ±0.01 deg C. Power meter readings at the zero and ambient load positions provide a calibration curve of power meter readings versus operating noise temperature. The computer commands the noise injecting diode to turn on and off in the ambient load and antenna positions, and performs calculations of system linearity, gain changes, and operating noise temperature. Calibrations are performed every 30 minutes or as often as commanded, and operating noise temperatures are computed every second or integrated over a desired time interval and then displayed on the screen and at the line printer. The data are automatically stored on the computer disk file.

For good operation for this particular Ka-band test package with respect to power meter resolution and system linearity, it was found that the input to the power meter sensor should be about 700 nanowatts when the waveguide switch was in the antenna path configuration. The adjustment of power levels was achieved with appropriate padding in the system and use of a variable IF attenuator in front of the power meter sensor.

Calibration and error analyses equations for the calibration method of this measurement system are based on

equations given in [3]. An option is available in the computer data reduction program to correct the measured operating noise-temperature values for nonlinearity [4]. More discussions of the calibration method and associated errors are given in Appendix A.

IV. Test Results

Figures 7(a) and 7(b) show examples of the overall system performance of the Ka-band test package on the ground at DSS 13 when the thermoelectric temperature controller was in operation. The symbols show data points for mini-calibrations performed every 30 min. During the 25-hr test period shown, the linearity factor remained nearly constant between 0.99 and 0.98. The gain factor varied between 1.00 and 0.99, which corresponds to a peak-to-peak gain change of only 0.04 dB. As may be seen in Fig. 7(b), the ambient-load physical temperature varied from a minimum of 2.7 to 16.1 deg C. Comparisons of the ambient-load physical temperature and gain factor plots show that they are correlated. Tests have shown that for ground tests, the outside air temperature and ambient-load physical temperatures track within a few deg C.

Noise-temperature symbols are used in the following equations, as well as in a table of results. For the reader's convenience, the symbols are defined in Table 1. When the test package is on the ground, the general expression for the operating noise temperature is

$$T_{op} = \frac{T'_{cb}}{L_{atm} L_{wg}} + \frac{T_{atm}}{L_{wg}} + T_{wg} + T_{hemt} + T_{fup} \qquad (1)$$

Under standard conditions at 32.0 GHz, the component values are $T'_{cb} = 2.0$ K, $T_{atm} = 7.02$ K, $T_{wg} = 17.67$ K, $T_{hemt} = 56.6$ K, $T_{fup} = 1.8$ K, $L_{atm} = 1.02683$ (corresponding to 0.1150 dB), and $L_{wg} = 1.06414$ (corresponding to 0.27 dB). Substitutions of the values into Eq. (1) result in a predicted T_{op} of 84.5 K.

Table 2 shows a tabulation of the Ka-band measurements for ground observations from October 12, 1990 through January 31, 1991. The grand average of the T_{op} values shown in Table 2 is 84.7 K, with a peak-to-peak deviation of $+1.6/-1.7$ K. The uncertainty associated with the grand average is estimated to be of 1.5 K (one standard deviation). This measured value of 84.7 K is in close agreement with the predicted value of 84.5 K.

Included in Table 2 are tabulations of the observation periods, the measured operating noise-temperature values, weather information, and normalized values after corrections were made for weather and the waveguide physical temperature values. This table shows the methodology used for normalizing zenith operating noise-temperature data to standard conditions. The normalized value of T_{op} is computed from

$$T_{op,n} = T_{op} + \frac{T'_{cb}}{L_{wg}} \left(\frac{1}{L_{atm,s}} - \frac{1}{L_{atm}} \right) + \frac{1}{L_{wg}} (T_{atm,s} - T_{atm}) + (T_{wg,s} - T_{wg}) \qquad (2)$$

where T_{op}, T_{atm}, T_{wg}, and L_{atm} are, respectively, the average measured T_{op}, computed T_{atm}, T_{wg}, and L_{atm} values given in Table 2. The values used for normalizing the measured values were $T_{atm,s} = 7.02$ K (for a 32-GHz Goldstone average clear atmosphere) and $L_{atm,s} = 1.02683$ (corresponding to 0.1150 dB). Other Ka-band (32.0 GHz) values used for normalizations were $T'_{cb} = 2.0$ K, $L_{wg} = 1.06414$ (corresponding to 0.27 dB), $T_{wg,s} = 17.67$ K for the above L_{wg}, and a standard physical waveguide temperature of 20 deg C.

At Ka-band, weather changes can cause significant variations in atmospheric noise contributions to operating noise temperatures. As may be seen in Table 2, the applications of weather corrections enabled significant improvements to be made to the operating noise temperatures for purposes of comparisons for measurements made at time periods separated by days and months.

Figure 8 shows curves of Ka-band atmospheric noise temperatures as functions of typical weather parameters during a calendar year at DSS 13. It is of interest to note that at Ka-band, typical weather conditions during the year at DSS 13 can cause the atmospheric noise temperatures to vary from 4.5 to 31.2, which represents a peak-to-peak variation of about 27 K. Method 1 of computer program SDSATM7M.BAS[1], described in [2], was the method used to derive values for Fig. 8. Method 1 was also used to make weather corrections for the noise temperature results presented in this article.

V. Concluding Remarks

Numerous Ka-band total-power radiometer tests on the ground showed that with a thermoelectric temperature

[1] Courtesy of S. D. Slobin of the Jet Propulsion Laboratory, Pasadena, California. SDSATM7M.BAS is a modified version of SDSATM4.BAS, but gives the same answers.

controller for the downconverter, gain changes were held to less than 0.2 dB over a 24-hour period, which is about as good as can be expected with a Ka-band total-power radiometer. Even when gain changes were large (before installation of the thermoelectric temperature controller), some of the gain instability problems were overcome by performing mini-calibrations more frequently than the normal 0.5-hr interval and by using the mini-calibration data to compute near-real-time corrections for gain changes. The combination of using a radiometer with small gain changes and performing more frequent mini-calibrations enabled better quality noise-temperature data to be obtained than was originally thought possible from a Ka-band total-power radiometer system.

Acknowledgments

The successful assembly and operation of the Ka-band test package are due to many people. D. Neff provided needed Ka-band parts and test equipment during critical phases of Ka-band test package testing. Although many difficulties were initially experienced with the Ka-band HEMT, these difficulties were overcome through the efforts of G. Ortiz, J. Loreman, L. Tanida, and S. Petty. The Ka-band downconverter was designed and fabricated by C. Risch and B. Finamore. Preliminary work on the Ka-band noise diode assembly was done by R. Strickland. All the above named are from the Radio Frequency and Microwave Subsystems Section.

The power supply and thermoelectric cooler for the downconverter were incorporated by R. Denning and R. Wetzel of the Microwave Observational Systems Section. Group Supervisor N. Yamane provided the technical and administrative support needed to get the thermoelectric assembly work done on a crash program basis at a critical phase of this Ka-band project. The thermoelectric cooler was the critical element that was needed to make the downconverter gain stable. C. T. Stelzried, of the TDA Technology Development Office, provided valuable consulting assistance on the subject of noise temperatures and radiometer calibrations.

Table 1. Definitions of symbols and abbreviations

Symbol	Definition
T_{cb}'	Effective noise temperature contribution to T_{op} from the cosmic background radiation, K. This value is a function of frequency and will differ from the actual cosmic background noise temperature of 2.7 K [5][a].
T_{cb}	Cosmic background radiation noise temperature, nominally 2.7 K
h	Planck constant
f	Frequency, Hz
k	Boltzmann constant
T_{atm}	Atmospheric noise temperature, K
T_{wg}	Noise temperature due to waveguide loss between the horn aperture and the input flange of the HEMT, K
T_{hemt}	Effective noise temperature of the HEMT as defined at the input flange of the HEMT, K
T_{fup}	Effective noise temperature of the follow-up receiver (downconverter + cables + power meter, etc.) as defined at the input flange of the HEMT, K
T_{op}	Operating noise temperature as defined at the input flange of the HEMT, K
RH	Relative humidity
HEMT	High-electron-mobility transistor
L_{wg}	Loss factor for the waveguide between the horn aperture and the input flange of the HEMT, power ratio > 1
L_{atm}	Loss factor of the atmosphere, power ratio > 1

[a] $T_{cb}' = T_{cb}\left[\frac{x}{\exp(x)-1}\right]$ where $x = \frac{hf}{kT_{cb}}$. (See details in [5].)

Table 2. Ka-band (32-GHz) measured zenith operating noise temperatures corrected for weather and waveguide noise changes. Ka-band test package is on the ground.

Observation	Average Measured T_{op}, K	Average Weather During Obsv.	Computed T_{atm}, K	Computed L_{atm}, ratio	Physical Waveguide Temp., deg C	T_{wg}, K	Normalized[a] T_{op}, K
10/12/90 DOY 285 0900–1250 UT	85.5	896.3 mb 17.9 deg C 15.8% RH	6.83	1.0258 (0.1104 dB)	18.9	17.61	85.7
11/09/90 DOY 313 1500 UT	87.5[b]	903.6 mb 14.9 deg C 31.7% RH	8.58	1.0324 (0.1386 dB)	15.0	17.38	86.3
01/19/91 DOY 019 1000–1500 UT	83.9	895.8 mb 7.12 deg C 44.3% RH	7.91	1.0303 (0.1296 dB)	6.7	16.88	83.9
01/31/91 DOY 031 0300–1000 UT	80.5	903.1 mb 5.3 deg C 13.7% RH	5.50	1.0211 (0.0906 dB)	1.3	16.55	83.0
							Grand average = 84.7 Peak deviations = +1.6/−1.7

[a] Normalized T_{op} values were computed through the use of Eq. (2).

[b] The Ka-band waveguide was cleaned and realigned in the test package.

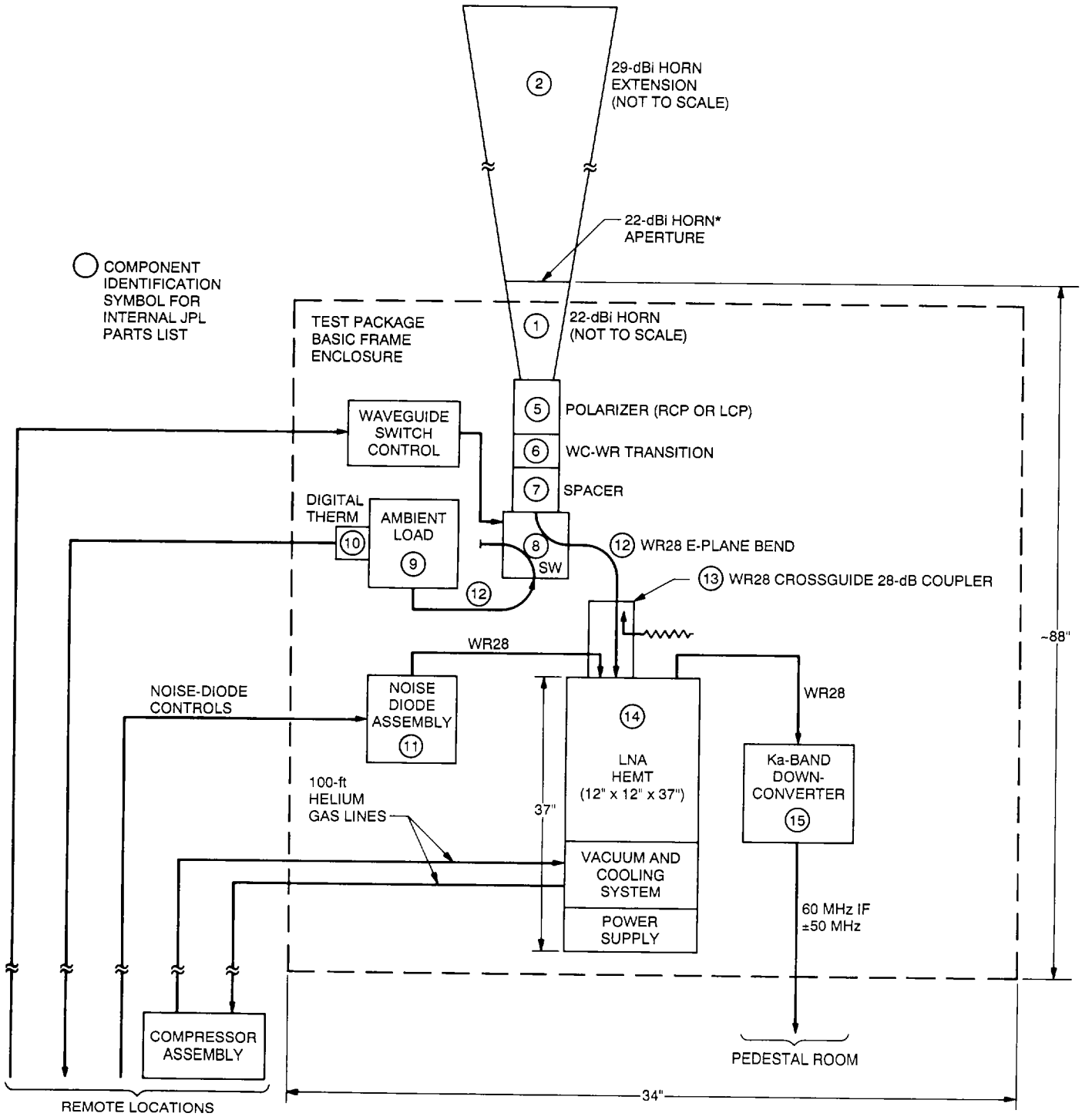

*ADDED A 0.375" LENGTH HORN EXTENSION AT THIS REFERENCE PLANE TO CONVERT FROM A 22-dBi TO 23-dBi HORN CONFIGURATION

Fig. 1. Ka-band test package system.

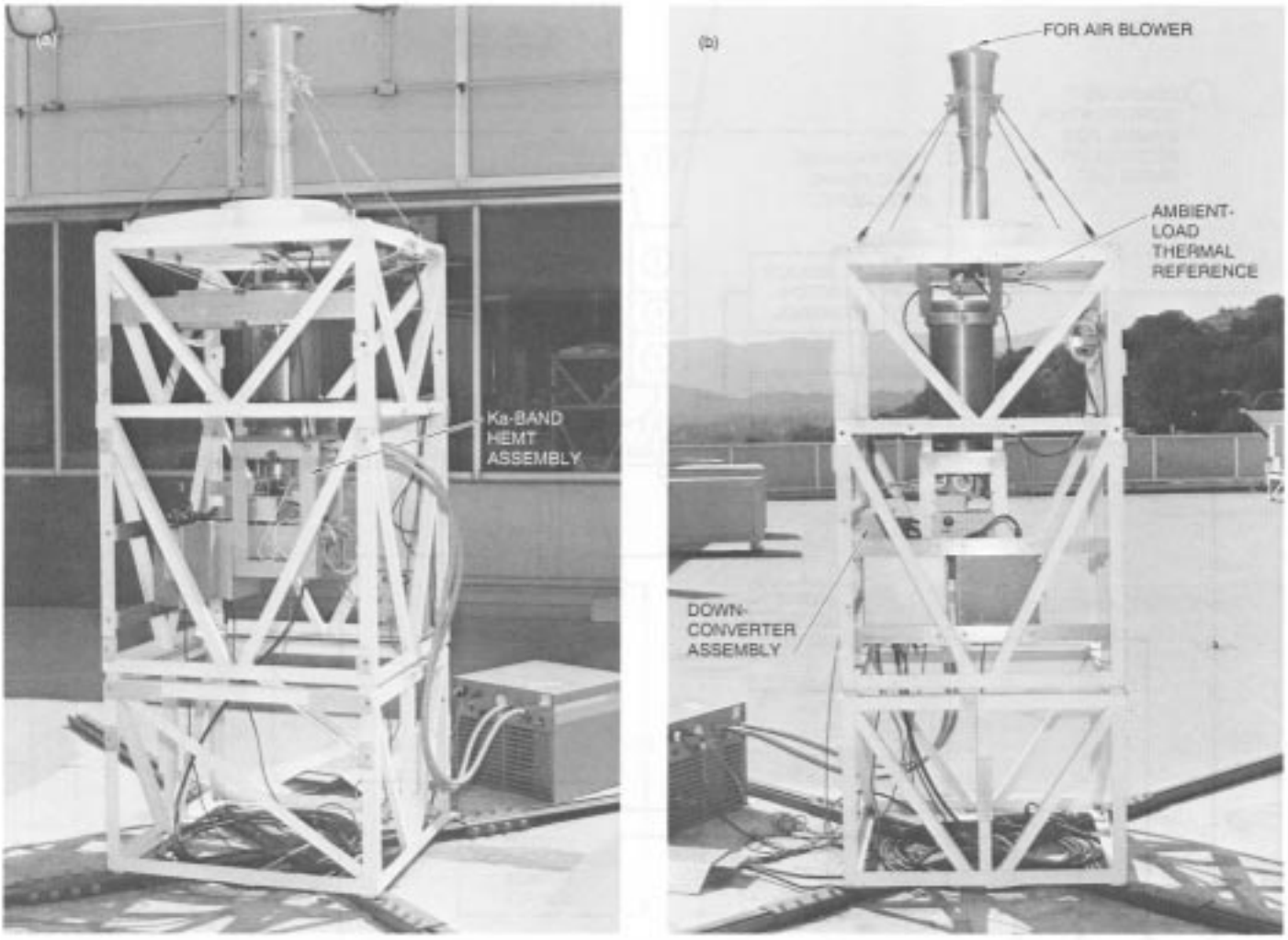

Fig. 2. Ka-band test package in its 29-dBi horn configuration for testing the system on the roof of the Telecommunications Building: (a) showing Ka-band HEMT and (b) showing Ka-band ambient-load thermal reference and downconverter.

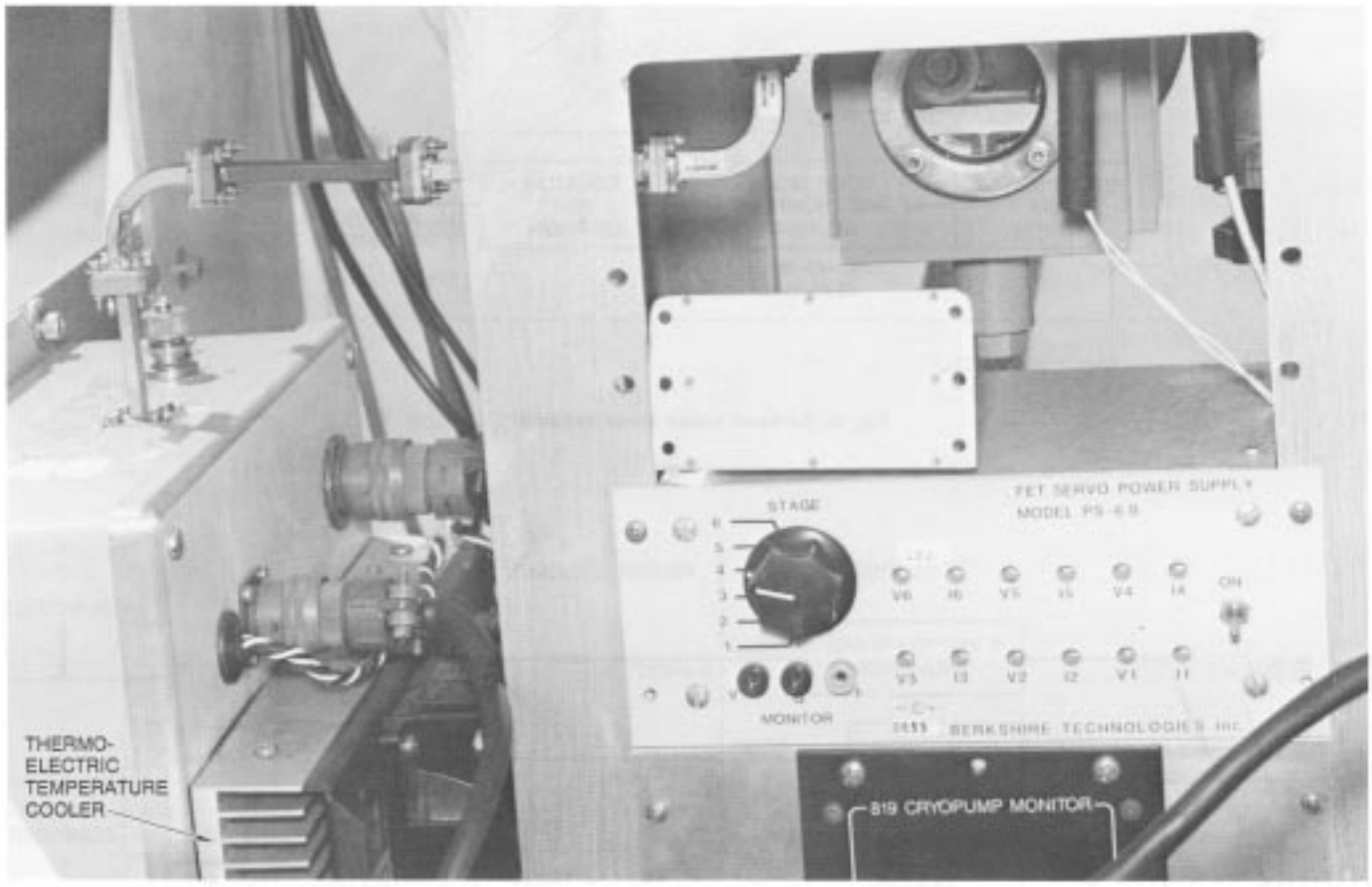

Fig. 3. Partial view of the post-HEMT assembly, including waveguide, downconverter, and thermal electric cooler assemblies.

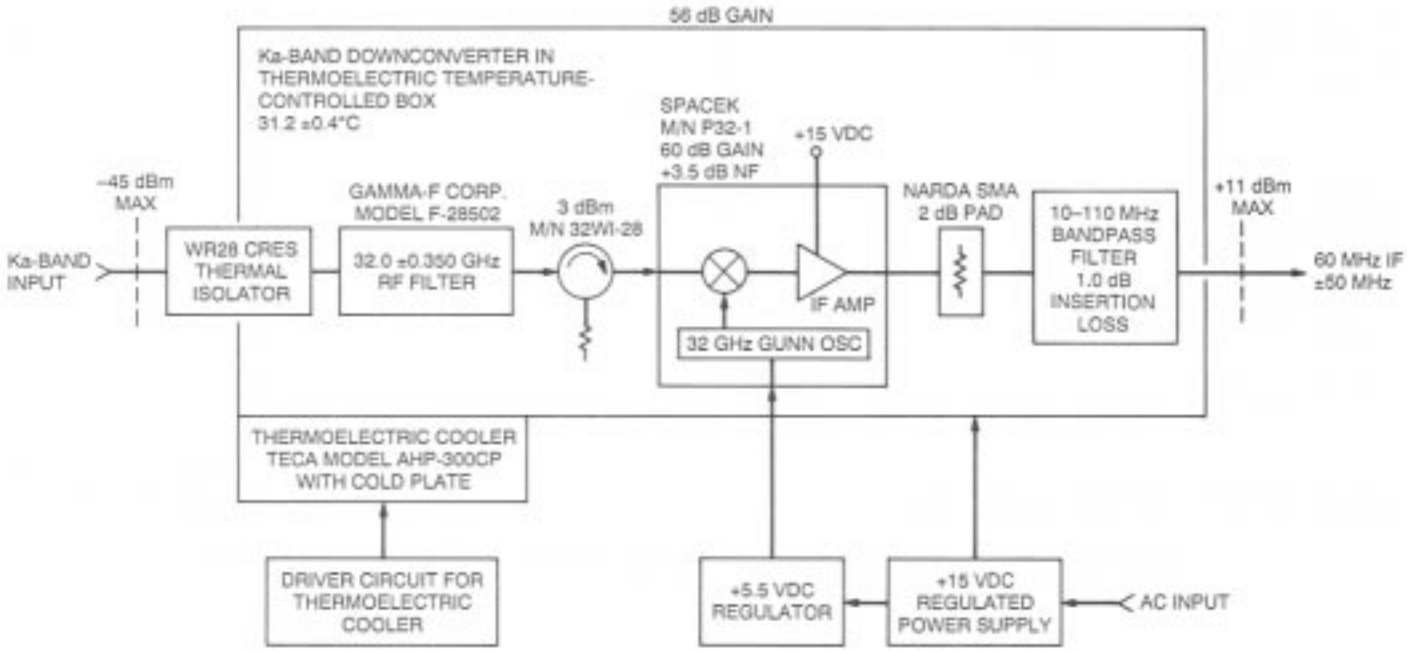

Fig. 4. Ka-band downconverter assembly.

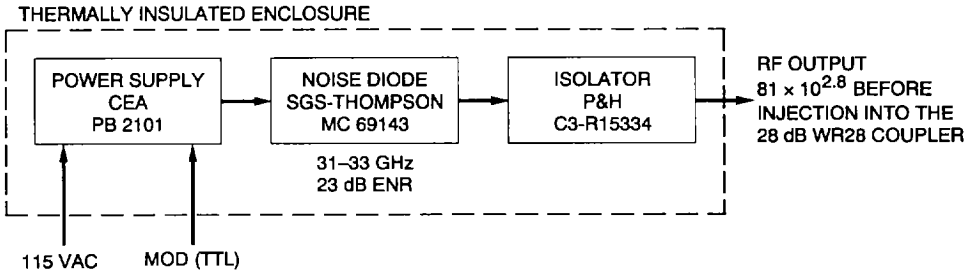

Fig. 5. Ka-band noise diode assembly.

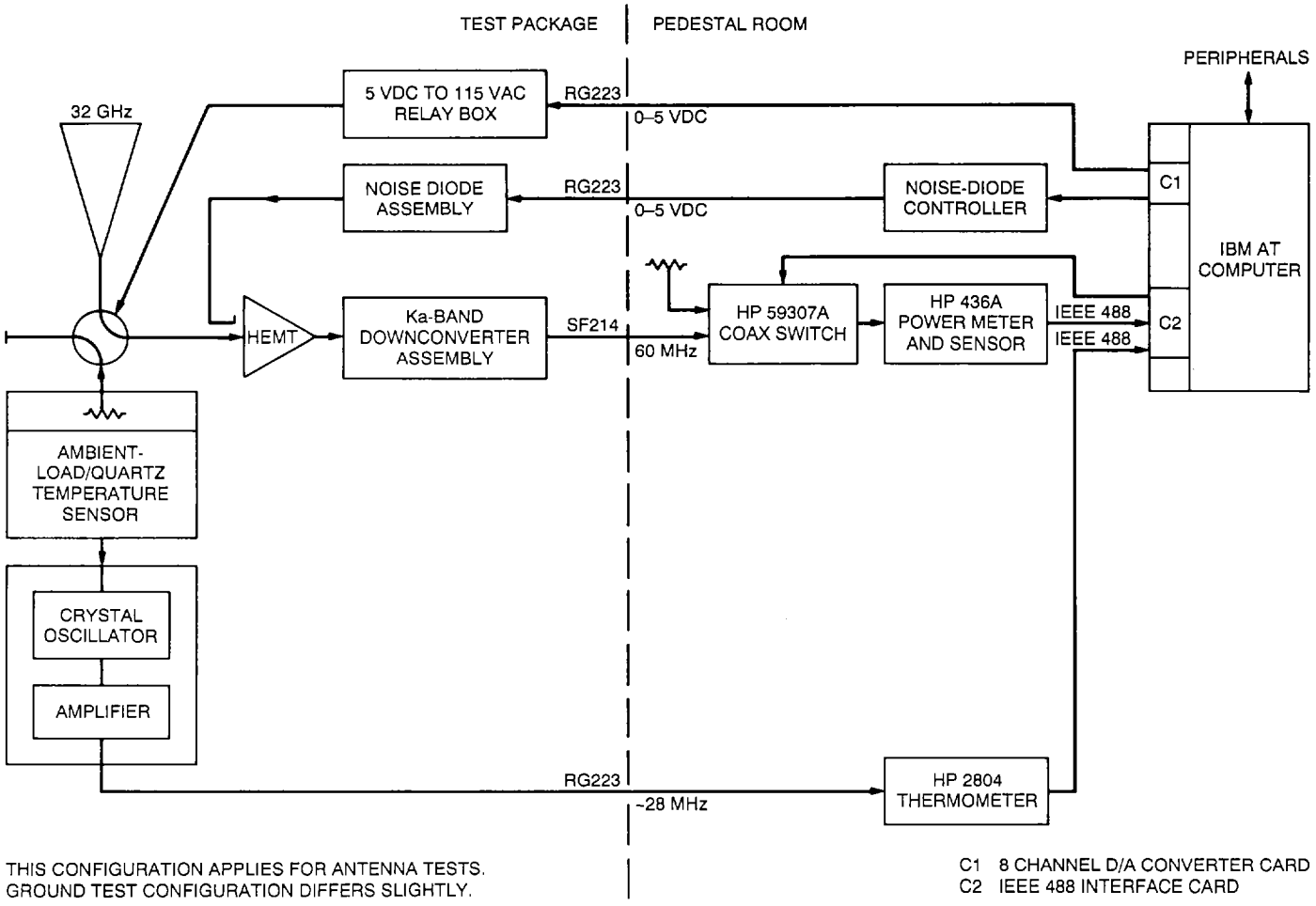

Fig. 6. The interface between the Ka-band test package and the total-power radiometer system.

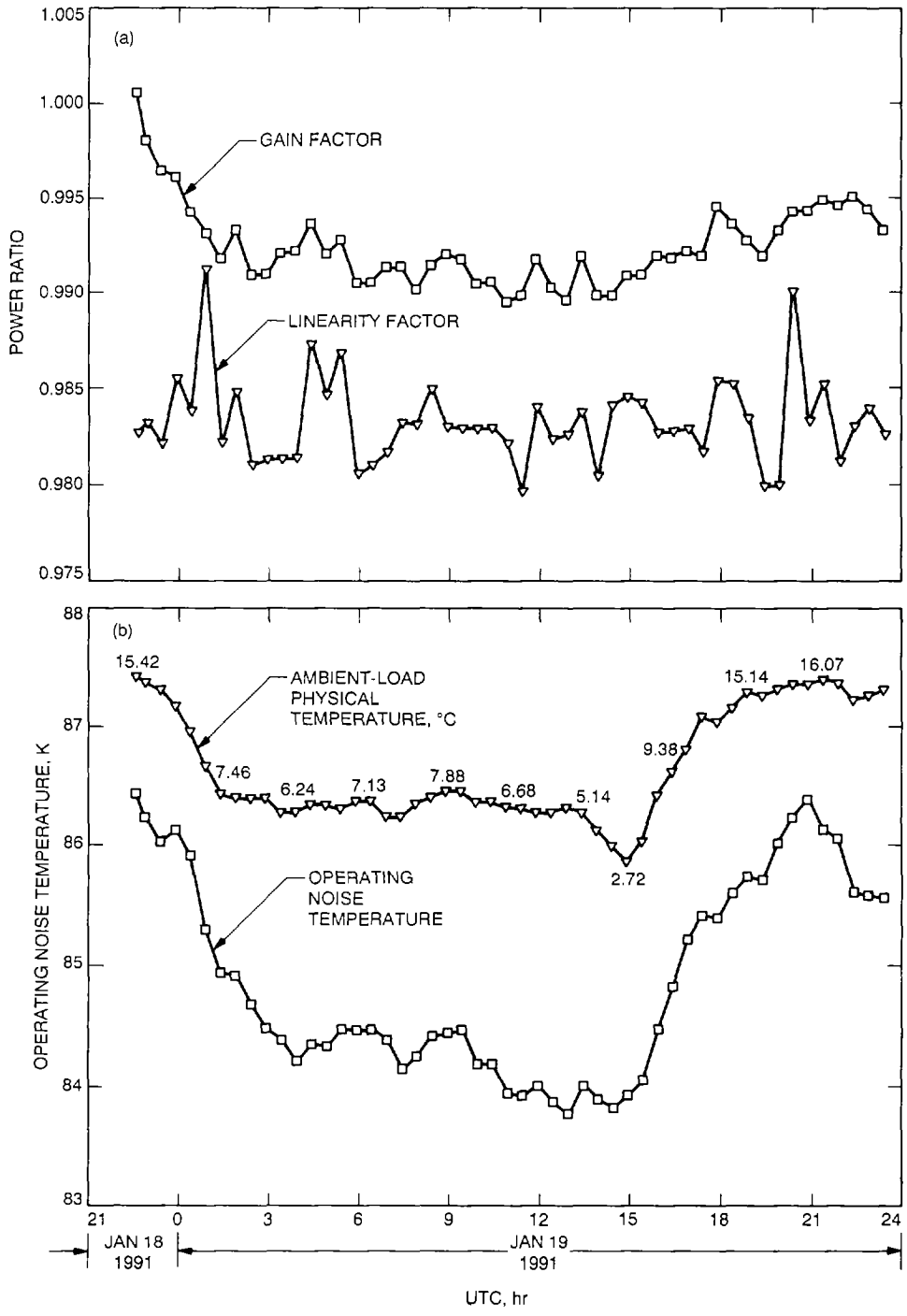

Fig. 7. Mini-calibration data during January 18 and 19, 1991. The Ka-band test package is outside of Building G60 (the Administrative and Laboratory building) at DSS 13: (a) gain and linearity factors and (b) operating noise and ambient temperatures.

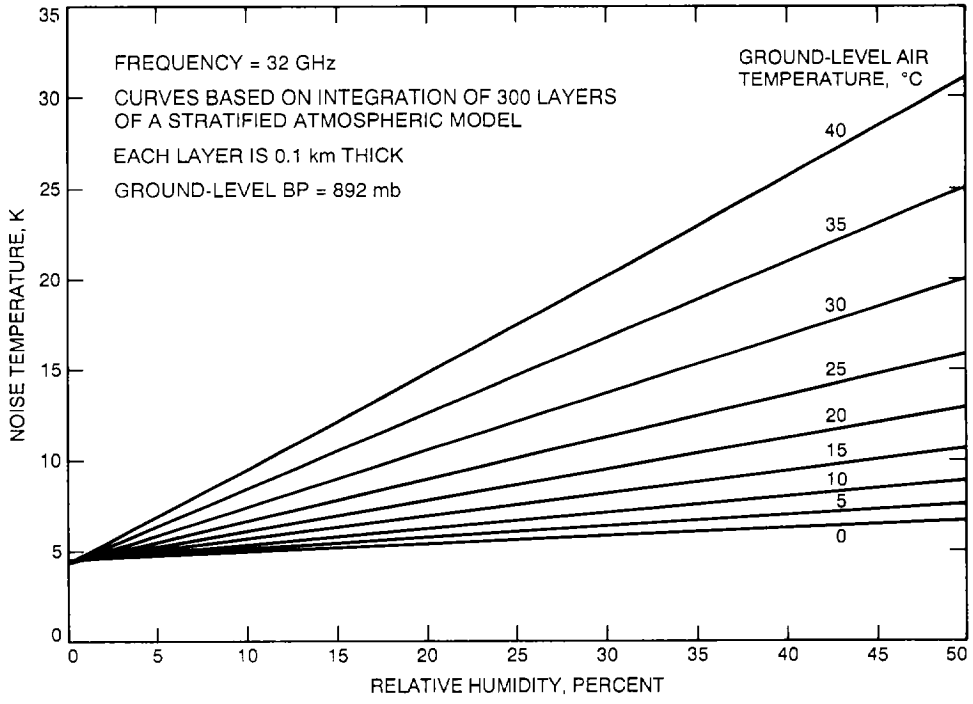

Fig. 8. Ka-band atmospheric noise-temperature contributions versus relative humidity and ground-level air temperature at DSS 13. (Courtesy of S. Slobin, Jet Propulsion Laboratory, Pasadena, California.)

Appendix A
Calibration Method and Error Analysis

This Appendix is written in response to numerous requests to describe the calibration system in more detail, and also to provide calibration and error analysis equations applicable to the test package noise-temperature measurement system. The measurement method and total-power radiometer equations follow those originally developed by Stelzried [3].

The principle of operation of the calibration system is illustrated in Fig. A-1. Two power meter readings are required to establish a linear power meter reading versus operating noise temperature calibration curve. The first required point of the curve corresponds to the power meter reading and an effectively zero[1,2] operating noise temperature when the power meter is zeroed by means of a remotely controllable coaxial switch that is terminated with a coaxial termination (Fig. 6). The second required point on the calibration curve corresponds to the power meter reading and the operating noise temperature when the waveguide switch is operated to be in the "ambient-load" path position (configuration). In this switch position, the waveguide ambient load becomes the input termination of the HEMT. The ambient load for this calibration system is used as the primary thermal noise reference standard. Based on the assumption that the calibration curve is linear, the two points are used to determine the constants (slope and intercept) of the calibration curve.

When the measurement system is used for measuring antenna operating noise temperatures, the waveguide switch is operated to be in the antenna path position. The power meter value is read by the computer and then the operating noise temperature (on the antenna) is computed from the power meter reading and the constants of the linear calibration curve.

It is assumed that the operating noise temperature in the ambient load configuration is well below the saturation point on the curve shown in Fig. A-1. A linearity check is accomplished by turning the noise diode on and off when the waveguide switch is first operated to be in the antenna path position and then to the ambient load path position. The excess noise due to the noise diode is computed and the difference of excess noise measured in the two switch positions provides a measure of the system's nonlinearity. An option in the computer program is provided for making corrections for nonlinearity through the use of equations derived by Stelzried in [4].

For purposes of performing an error analysis of the measured value of the operating noise temperature (on the antenna), the following calibration equations are applicable. It should be pointed out that in the main body of this article, T_{op} was used to denote the operating noise temperature in the antenna configuration. In the analysis below, T_{opa} and T_{oph} are used to denote operating noise temperatures for the antenna and ambient-load system configurations. The following general equations are applicable to the X- or Ka-band test package noise-temperature measurement systems:

$$T_{opa} = T_{oph}\frac{P_{opa}}{P_{oph}} \tag{A-1}$$

$$T_{oph} = T_{pc} + 273.16 + T_e \tag{A-2}$$

$$T_e = T_{hemt} + T_{fu} \tag{A-3}$$

where many of the symbols have already been defined elsewhere in this article. Definitions for symbols not previously defined are T_{pc} = ambient load physical temperature in deg C, P_{oph} = power meter reading in nW when the waveguide switch is in the ambient-load path position, and P_{opa} = power meter reading in nW when the waveguide switch is in the antenna path position.

For this particular calibration technique to be useful in practice, it is required that T_e be known accurately at the HEMT input flange, where T_e is defined above by Eq. (A-3). For T_e to be known accurately, it is necessary for T_{hemt} to be measured extensively in the laboratory prior to the installation of the HEMT assembly into the test package. Furthermore, it is assumed for this calibration method that T_{hemt} does not change with time or with test package motions or antenna motions. It has been found, based on two or more years of operation in the field, that T_{hemt} does not change significantly with time or antenna motion and the above assumptions are valid ones. Hence, the cooled HEMT is an ideal low-noise amplifier to

[1] Typically, this reading is less than 3×10^{-4} K for a system having an overall gain of 60 dB. The exact value can be calculated from an equation given by Stelzried[2].

[2] C. T. Stelzried, "DSS 13 Radiometer System Status and Performance," Interoffice Memorandum CTS-90-001 (internal document), Jet Propulsion Laboratory, Pasadena, California, January 30, 1990.

use for the noise measurement technique employed for the test package calibration system. The follow-up receiver noise temperature contribution (as defined at the HEMT input) is usually measured after installations through the use of a Y_{on-off} method. This follow-up noise temperature contribution is also required to be constant with time. If the HEMT gain is sufficiently high (> 30 dB) and the follow-up receiver effective input noise temperature is less than 500 K, the follow-up receiver contribution will be less than 0.5 K. Therefore, there is less probability that instabilities in the operating noise temperature measurements will come from the follow-up contribution.

Another requirement for the calibration system is that the ambient-load physical temperature T_{pc} can be measured to a high degree of accuracy (better than 0.2 deg C). If the requirements for both T_e and T_{pc} are met, then updated measurements of T_{pc} enable updated values of T_{oph} to be calculated and enable gain changes in the radiometer system to be isolated. Then, corrections can be determined for *gain changes* and applied to raw (uncorrected) measured operating noise temperature values to obtain what the computer program has labeled as "corrected system temperatures." Unfortunately, this terminology has caused some confusion in data comparison because Stelzried [4] also uses the same term to mean an operating noise temperature corrected for both *gain changes* and *nonlinearity*. The process of obtaining updated values of T_{pc} and corrected T_{op} is accomplished automatically at any desired periodic interval or instantaneously upon command by an experimenter through the use of a single computer keystroke operation. The procedure for obtaining data for an updated noise temperature calibration curve (Fig. A-1), making corrections for gain (and linearity, if desired), is referred to as a "mini-cal" (mini-calibration) operation[2].

If T_e is not known accurately or changes with time, the errors produced on the measurement of T_{op} can be calculated from the equations given below. Errors caused by other error sources, such as uncertainties of the ambient-load physical temperatures and power-meter reading errors can be calculated from the error analysis equations presented below.

Following the method given in [3], the root sum square (rss) of the individual error contributions to the overall T_{opa} measurement error is

$$E_{Topa} = \mathrm{SQRT}(E^2_{Topa/Tpc} + E^2_{Topa/Te} + E^2_{Topa/Popa} + E^2_{Topa/Poph} + E^2_{Topa/mm}) \quad \text{(A-4)}$$

where SQRT denotes square root and the general symbol of the form $E_{y/x}$ is used to denote the error in the value of y due to an error in x.

Then,

$$E_{Topa/Tpc} = \left|\frac{\partial T_{opa}}{\partial T_{pc}} E_{Tpc}\right| = \frac{T_{opa}}{T_{oph}} E_{Tpc} \quad \text{(A-5)}$$

$$E_{Topa/Te} = \left|\frac{\partial T_{opa}}{\partial T_{e}} E_{Te}\right| = \frac{T_{opa}}{T_{oph}} E_{Te} \quad \text{(A-6)}$$

$$E_{Topa/Popa} = \left|\frac{\partial T_{opa}}{\partial P_{opa}} E_{Popa}\right| = \frac{T_{oph}}{P_{oph}} E_{Popa} \quad \text{(A-7)}$$

$$E_{Topa/Poph} = \left|\frac{\partial T_{opa}}{\partial P_{oph}} E_{Poph}\right| = \frac{T_{opa}}{P_{oph}} E_{Poph} \quad \text{(A-8)}$$

Equations for $E_{Topa/mm}$ are involved and will not be presented in this Appendix. Computer programs for a personal computer have been written for the mismatch error equations given by Otoshi [6]. Sufficiently good estimates of the worst-case errors due to mismatch can be obtained through the use of simplified error formulas given in [3].

In the above, it can be seen that in order to minimize the error on the measurement of T_{opa}, it is desirable to make the ratio of T_{oph}/T_{opa} as large as possible. This goal is achieved in practice by selecting an accurate hot reference load noise temperature that is much higher than the antenna noise temperature to be measured and by using a receiver with a low value of T_e. For the case where the ambient reference termination provides the hot-source reference noise temperature, it is desirable that the ambient-load operating-noise temperature be at least 10 times higher than the antenna operating-noise temperature. Examples of X- and Ka-band test package error calculations are given in Table A-1.

Table A-1. Examples of errors in measurement of antenna operating noise temperature

	X-Band	Ka-Band
Measured or known parameter values		
T_{opa}	30 K	87 K
T_e	13.4 K	58.4 K
T_p	293.16 K	293.16 K
T_{oph}	306.56 K	351.56 K
P_{opa}	700 nW	700 nW
P_{oph}	7153 nW	2829 nW
1σ estimate of individual error sources		
E_{Tpc}	0.2 deg C	0.2 deg C
E_{Te}	0.2 K	0.5 K
E_{Popa}[a]	2.4 nW	2.4 nW
E_{Poph}[a]	15.3 nW	6.7 nW
Error source contributions		
$E_{Topa/Tpc}$	0.02 K	0.05 K
$E_{Topa/Te}$	0.02 K	0.12 K
$E_{Topa/Popa}$	0.10 K	0.30 K
$E_{Topa/Poph}$	0.06 K	0.21 K
T_{opa} rss error	0.12 K	0.39 K

[a] Assume that the power meter accuracy in nanowatts is given by $\pm(1 + 0.002 \times \text{PMR})$, where PMR is the power meter reading in nanowatts.

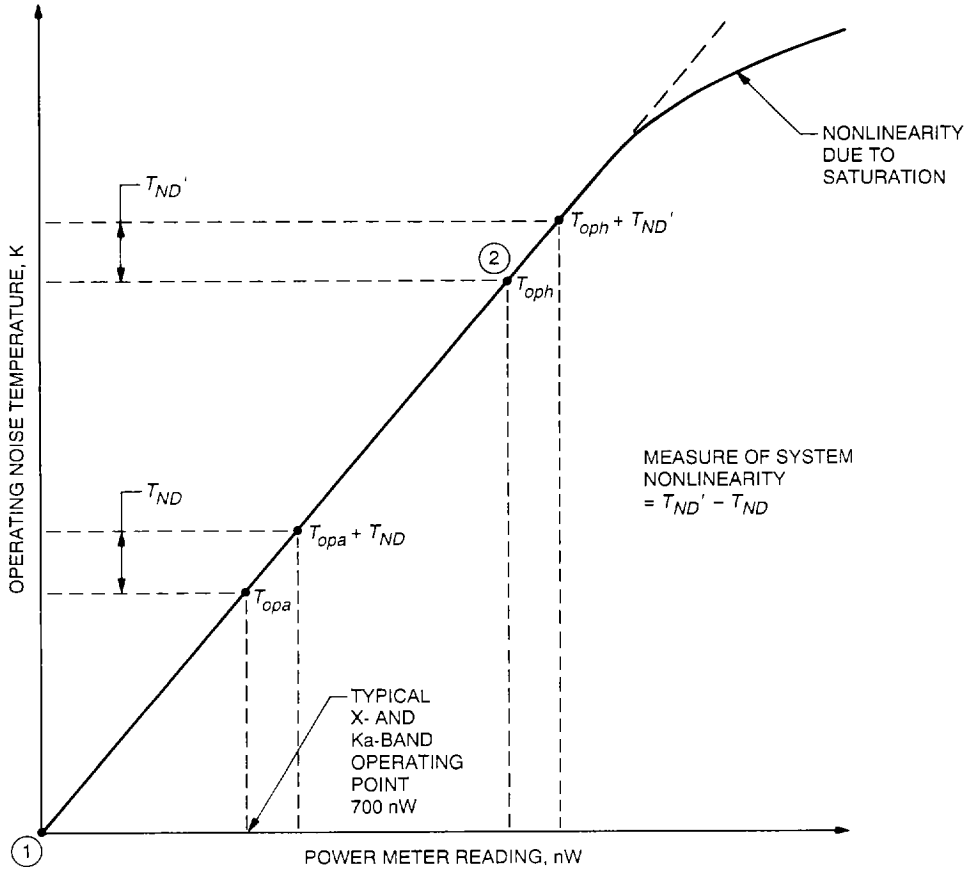

Fig. A-1. Example of a calibration curve for X- or Ka-band test package radiometer system.

References

[1] T. Y. Otoshi, S. R. Stewart, and M. M. Franco, "A Portable X-band Front-End Test Package for Beam-Waveguide Antenna Performance Evaluation—Part I: Design and Ground Tests," *TDA Progress Report 42-103*, vol. July–September 1990, Jet Propulsion Laboratory, Pasadena, California, pp. 135–150, November 15, 1990.

[2] T. Y. Otoshi, S. R. Stewart, and M. M. Franco, "A Portable X-band Front-End Test Package for Beam-Waveguide Antenna Performance Evaluation—Part II: Design and Ground Tests," *TDA Progress Report 42-105*, vol. January–March 1991, Jet Propulsion Laboratory, Pasadena, California, pp. 54–68, May 15, 1991.

[3] C. T. Stelzried, "Operating Noise-Temperature Calibrations of Low-Noise Receiving Systems," *Microwave Journal*, vol. 14, no. 6, pp. 41–46 and 48, June 1971.

[4] C. T. Stelzried, "Non-linearity in Measurement Systems: Evaluation Method and Application to Microwave Radiometers," *TDA Progress Report 42-91*, vol. July–September 1987, pp. 57–61, November 15, 1987.

[5] C. T. Stelzried, "The Deep Space Network—Noise Temperature Concepts, Measurements, and Performance," JPL Publication 82-33, Jet Propulsion Laboratory, Pasadena, California, pp. 2-1–2-3, September 15, 1982.

[6] T. Y. Otoshi, "The Effect of Mismatched Components on Microwave Noise Temperature Calibrations," *IEEE Transactions on Microwave Theory and Techniques (Special Issue on Noise)*, vol. MTT-16, no. 9, pp. 675–686, September 1968.